A&A manuscript no.
(will be inserted by hand later)

Your thesaurus codes are:
06.16.3, 06.20.1, 02.13.2, 02.18.7

ASTRONOMY AND ASTROPHYSICS
August 5, 1999

The energy balance in solar prominences

U. Anzer[1] **and P. Heinzel**[2,1]

[1] Max-Planck-Institut für Astrophysik, Karl-Schwarzschild-Str. 1, D-85740 Garching, Germany
[2] Astronomical Institute, Academy of Sciences of the Czech Republic, CZ-25165 Ondřejov, Czech Republic

Received; accepted

Abstract. In this paper we study the energy balance in quiescent solar prominences. For this investigation we use a simple 1D slab model in magneto-hydrostatic equilibrium. We divide the studied region into two parts:
The inner region consisting of the prominence itself and the cool part of the transition region (up to 30000 K). In this region the plasma is optically thick in several atomic transitions and therefore we have to solve the non-LTE radiative transfer problem in this part. This allows us to derive self-consistently the gas density, the ionization degree of hydrogen and the hydrogenic radiation losses. The energy transport by thermal conduction can be neglected in this region.
In the outer part of the transition region, the thermal conduction becomes very important but the treatment of radiation is simplified by the fact that the plasma is optically thin.
We find that energy balance in prominences can only be obtained for special forms of the heating function. This requirement is very stringent for the inner parts, while in the outer region thermal conduction can transport large amounts of the heat energy and therefore a wider class of heating functions will be allowed.

Key words: Sun: prominences, MHD, Radiative transfer, Energy balance

1. Introduction

The existence of quiescent solar prominences gives rise to many interesting questions. These structures extend high into the solar corona, they have a small width compared to their length and height, they live for a long time and show only modest flow velocities. These facts imply that they have to be close to a state of mechanical equilibrium, at least the structure as a whole. This equilibrium problem has been investigated by many authors for the last fourty years. Recent summaries of these attempts to construct equilibria can be found for example in Tandberg–Hanssen (1995) and Webb et al. (1998). It seems that the basic support mechanism is now reasonably well understood, but there remain many open questions concerning the formation, the stability, the fine structure and the internal flows of these prominences. The requirement of a mechanical equilibrium, however, is not the only necessary condition for the existence of prominences. In addition to this there is also the need for a detailed energy balance in those structures.

Early attempts to obtain an energy balance for quiescent prominences were made by Poland & Anzer (1971). They used a simplified version of the Kippenhahn & Schlüter (KS) model and calculated the emission from the optically thick prominence. The integrated radiative losses obtained were of the order of 10^5 erg s^{-1} cm^{-2}. The authors suggested that these losses can be balanced by total conductive inflow of thermal energy from the surrounding hot corona. However, several open questions remained concerning the *local* energy balance. The authors did not take into account the radiative losses from the prominence–corona interface, which can be quite large and therefore will require additional heating. Another problem with such a model is the fact that the conductive flux can not penetrate deep enough into the prominence because the conductivity is very low at central prominence temperatures. A third point is that the additional heating has been left out completely. Therefore this kind of models is far from being complete.

Heasley & Mihalas (1976) (hereafter referred to as HM) have studied the radiative properties of the hydrogen plasma in quiescent prominences. They also used KS-type magnetostatic models and the energy balance problem was reduced to radiative equilibrium (their models M1 to M3). As a result the central temperatures are rather low, below 5000 K for their models M2 and M3. HM also found that the prominence width for these magnetic equilibrium models is rather small, ranging from 170 km to 860 km. The reason for this result lies in the very large value assumed for the coronal pressure ($p_0 = 0.56$ dyn cm^{-2}) and the value taken for the horizontal field strength (10 G). If p_0 is reduced sufficiently (values of 0.01 to 0.02 dyn cm^{-2}

Send offprint requests to: U. Anzer
ula@mpa-garching.mpg.de

seem reasonable) then low mass prominences can be considerably wider. The very massive prominences will always be quite narrow; their width can only be increased if the horizontal field becomes very large. For some other models they consider an energy balance between the radiative losses and some form of mechanical heating. They used a heating function given by $H = h\rho$ with $h = (1{-}6)\times 10^9$ erg s^{-1} g^{-1} and ρ being the gas density. These models are not in a magnetic equilibrium, HM use isobaric slabs which are confined by a large coronal pressure. They assume coronal pressures between 0.13 and 0.26 dyn cm^{-2} which are an order of magnitude larger than typical coronal values, and the discrepancy with respect to the observations becomes even larger when one takes into account that prominences are usually surrounded by cavities of low coronal density. The heating which is required in these models is of the order of 10^{-3} erg s^{-1} cm^{-3} which is also very high. It is therefore questionable to what extend these models can describe real prominences.

Analytical models for prominences in mechanical and energy equilibrium were developed by Low & Wu (1981). They assumed a very special form for the radiative loss function and obtained models with central temperatures around 28000 K. Therefore, such models are not relevant to studies of the inner parts of prominences.

Chiuderi & Chiuderi Drago (1991) studied the transition region around prominences by using a very general form of the energy equation with the radiative losses treated in the coronal approximation. They also took into account the thermal shielding by inclined magnetic fields. These authors showed that the observed difference in radiative output between the sides and the top of the prominence (seen as a filament) can be explained by the orientation of the magnetic field in the prominence region with respect to the temperature gradients. Chiuderi Drago et al. (1992) modeled the transition regions which could be present around thin horizontal magnetic flux tubes.

Finally, Fontenla et al. (1996) (hereafter referred to as FRVG) developed a model for prominences which consist of many extremely thin parallel sheets. They assumed a balance between radiative losses and gains resulting form thermal conduction in which also the ambipolar diffusion was included. FRVG only considered isobaric configurations and found that such equilibria are possible if the region in which the temperature rises from 6500 K to 10^5 K is sufficiently narrow. If the pressure is 0.02 dyn cm^{-2} the width amounts to about 340 km and for 0.2 dyn cm^{-2} it decreases to less than 40 km. But neither the mechanical equilibrium nor any effects due to some additional heating are considered in this investigation.

As can be seen, different aspects of the mechanical and energy balance have been studied in the past, but none of the models so far developed takes into account self-consistently both these equilibria on scales ranging from the central cool parts of the prominence into the corona. In the present paper we investigate the energy balance for 1D models which are in magnetostatic equilibrium. We consider the entire prominence region consisting of the cool interior as well as the transition region between prominence and corona. In Sect. 2 we describe the model used and the basic energy equation. In Sect. 3 we describe the pressure and temperature structure in the inner cooler parts, while Sect. 4 and 5 are devoted to non-LTE models of those parts. In Sect. 6 we model the transition region. The conclusions which we derive from our models are presented in the last section.

2. Basic assumptions and the energy balance equation

For our exploratory investigation we use a 1D slab model of the prominence. We therefore ignore all possible prominence fine structures and the consequences resulting from inhomogeneities. For this reason our results will describe the averaged behaviour of real solar prominences. However, slabs having small dimensions of the order of several hundreds km can be considered as prototypes of the fine-structure threads. In another paper (Heinzel & Anzer 1999) we investigate individual threads as 2D vertical structures in magnetostatic equilibrium.

For our modelling we use a standard coordinate system for which the x–direction is perpendicular to the slab, the y–direction along it and the z–direction oriented vertically upward. The magnetic equilibrium is given by a generalised Kippenhahn-Schlüter model with prescribed temperature variation (see next section). For typical values of the field strength and column mass the magnetic field will have sizeable dips and therefore the gas pressure inside the prominence will vary substantially. On the other hand, the transition region is treated as an isobaric configuration because in general the length-scale for temperature variation, given by $T/(dT/dx)$, is much smaller than the local pressure scale height everywhere in this transition region. We shall also assume a uniform magnetic field in the transition region. This is a good approximation only as long as the size of the magnetic arcade is sufficiently larger than the width of the transition region. In this investigation we shall divide the prominence configuration into two parts and model them separately. There is the inner cool and dense region, and the transition region with modest to high temperatures (the prominence-corona transition region – PCTR). The inner region is optically thick and since the temperature is low and gradients are small, the thermal conduction can be neglected. In the outer region, on the other hand, the effects of conduction will be quite large. In that part all radiation can be treated by the optically thin approximation.

In 1D models the equation of energy balance can be written as

$$B_x \frac{d}{dx}\left(\frac{B_x}{B^2}\kappa T^{5/2}\frac{dT}{dx}\right) = L - H \tag{1}$$

where the left-hand side is the divergence of the conductive flux, with $B^2 = B_x^2 + B_y^2 + B_z^2$ and κ being the Spitzer conductivity coefficient. L represents the radiative losses, i.e. the difference between emitted and absorbed radiation, and H includes all types of additional heating occuring in this region (wave heating, enthalpy flux, magnetic reconnection etc.). So far no generally accepted form for this heating function has been presented. In our modelling the conductive flux is only in the direction of the magnetic field; the flux perpendicular to the field is neglected for two reasons: inside the cool part even the parallel flux is negligible, and in the PCTR the ionization degree is very high.

FRVG found that the ambipolar diffusion can enhance the efficiency of the thermal conduction. This effect, however, is only significant at temperatures where hydrogen is partially ionized (say below 30000 K). For the central prominence temperature of 6500 K the effective conductivity lies about a factor 100 above the conventional Spitzer conductivity term (see FRVG), provided that the threads are very narrow.

The boundary between prominence interior and transition region in our modelling approach is given by the requirement that inside the interior some of the hydrogen transitions are optically thick (namely the Lyman lines) whereas the PCTR is optically thin. We specify this boundary by prescribing a fixed value for the temperature at the boundary (see below).

3. Central parts of the prominence and the base of PCTR

As mentioned before, for the inner cool part of the prominence we consider the KS-type pressure equilibrium with a prescribed temperature. By the cool part we mean here the central parts of the prominence (1D slab in the present case) which radiate in optical lines, surrounded by the base of the prominence-corona transition region (PCTR) with the kinetic temperature rising to 30000 K. This rather arbitrary temperature limit was chosen in order to describe accurately the hydrogen L α line formation. Above this temperature, the radiation losses approach approximately the optically-thin limit. On the other hand, our coronal plus PCTR part of models is limited by the temperatute 20000 K where the conductive heating is already small. In this way we have a fairly smooth transition between cooler and hotter parts of our models, although the region between 20000 and 30000 K should not be considered too literaly, in fact it could also be shifted to somewhat higher temperatures.

3.1. Pressure equilibrium

The pressure balance in KS-type models can be expressed as function of the column mass m (HM; Heinzel & Anzer, 1998)

$$p(m) = 4p_c \frac{m}{M}\left(1 - \frac{m}{M}\right) + p_0 \tag{2}$$

where

$$dm = -\rho dx. \tag{3}$$

ρ is the gas density and p_0 represents the gas pressure at the outer boundary (PCTR or coronal gas pressure which we take to be constant). The column mass m extends from $m = 0$ at one surface to $m = M$ at the other one. For M we get

$$M = \frac{B_x B_{z1}}{2\pi g}, \tag{4}$$

where B_x and B_{z1} are the components of the magnetic-field vector at the slab boundary and g is the gravitational acceleration on the solar surface. Note that we take $B_x =$ const. throughout the prominence, B_z varies together with the density (see Anzer 1995), while B_y does not affect the equilibrium and is the measure of the magnetic field shear - here we set $B_y = 0$ for simplicity. p_c is defined as

$$p_c = \frac{B_{z1}^2}{8\pi} \tag{5}$$

(see Heinzel & Anzer, 1998). From these equations we get the central gas pressure

$$p_{cen} = p_c + p_0 \tag{6}$$

and the mean gas pressure

$$\overline{p} = \frac{1}{M}\int_0^M p\, dm = \frac{2}{3}p_c + p_0. \tag{7}$$

Note that in Anzer (1995) and in Anzer & Heinzel (1998), the coronal gas pressure p_0 is neglected and thus $p_{cen} = p_c$, while in Heinzel and Anzer (1998) it is consistently accounted for (although there p_c was misleadingly called the central gas pressure).

Similarly one can define a mean gas density by the relation

$$\overline{\rho} = \frac{1}{M}\int_0^M \rho\, dm, \tag{8}$$

and from this a typical value for the slab thickness is obtained as

$$D = \frac{M}{\overline{\rho}}. \tag{9}$$

One finds that this thickness D is considerably smaller than the extension of the whole inner region which amounts to

$$D_{tot} = \int_0^M \frac{dm}{\rho} \tag{10}$$

and contains the prominence interior and the base of the PCTR, i.e. our 'cool part' of the model.

3.2. Temperature structure

The advantage of our formulation is that the pressure balance equation on the m-scale is independent of the temperature structure, which is not true for the x-scale (compare with Poland & Anzer, 1971). To describe the temperature structure of the inner part of the prominence, one should in principle solve the energy-balance Eq. (1). However, in the inner cool part, the temperature gradients are expected to be very small compared to those in the PCTR (even if ambipolar diffusion is included) and thus we neglect the thermal conduction term which is justified by our results presented below. The energy balance equation then reduces to

$$L - H = 0. \tag{11}$$

If we further neglect all heating terms ($H = 0$), we get the condition that the radiative losses L are zero everywhere, which means the radiative equilibrium (RE) condition. Configurations in RE were calculated by HM in connection with KS pressure balance and these authors have arrived at very low temperatures at the prominence center. Furthermore, the radiative equilibrium does not produce any PCTR-like temperature increase, which definitely requires extra heating. The models of HM are thus not relevant to our problem. FRVG also neglect the H-term and they balance the radiation losses by conductive heating and ambipolar diffusion, even in the cool core. Since they fix the central temperature to 6500 K, which is much higher than the RE temperatures of HM, their conductive heating terms require rather large temperature gradients in the core and this leads to very narrow cool parts which are much below our present instrumental resolution.

Since we consider the conductive heating and that due to ambipolar diffusion quite neglibible for slabs of reasonable widths and column masses, the energy equation in the cooler part should reduce to Eq. (11). However, we can not prescribe a depth variation of H because the physical nature and the individual components of this heating term are largely unknown. Therefore, rather than specifying H, we prescribe the temperature profile of the slab, which is more or less consistent with a large amount of observational temperature diagnostics based on various spectral data. Prescribing the temperature thus means that we use here a kind of 'semiempirical' approach to modelling, although we do not directly compare our synthetic spectra with observations.

For the central part we take two representative temperatures, $T_{cen} = 6500$ K as in FRVG and $T_{cen} = 8000$ K as in Anzer & Heinzel (1998) and Heinzel & Anzer (1998). Both lie well in the range of the 'Hvar Reference Atmosphere of Quiescent Prominences' (Engvold et al. 1990). To reach the boudary transition-region temperature $T_{tr} = 30000$ K, we use a functional dependence on the column mass m which satisfies the symmetry of the 1D slab (as for pressure in Eq. (2)) given by

$$T = T_{cen} + (T_{tr} - T_{cen}) \left[1 - 4\frac{m}{M}\left(1 - \frac{m}{M}\right)\right]^{\gamma}, \tag{12}$$

with $\gamma \geq 2$.

4. Non-LTE models and radiation losses

Having defined the basic structural parameters and their dependence on m, we can construct non-LTE models of the cool part of the prominence. As input quantities we use the total column mass M, the central temperature T_{cen}, the boundary temperature T_{tr}, the mean gas pressure $\overline{p}$ (which agrees with typical observations), the coronal gas pressure p_0 and the microturbulent velocity $v_t = 5\ \mathrm{km\ s^{-1}}$. In order to obtain a realistic gas density, we use a mixture of hydrogen and helium with a helium abundance $\alpha = 0.1$. However, only the hydrogen ionization is supposed to contribute to the electron density. The height of the prominences was taken to be 30000 km above the solar surface and this defines the dilution of the incident solar radiation. The input parameters are summarized in Table 1, where T6 means $T_{cen} = 6500$ K and T8 means $T_{cen} = 8000$ K.

For the solution of the non-LTE problem (radiative transfer and statistical equilibrium equations) we use the MALI technique as described for prominences by Heinzel (1995) and Paletou (1995). Since we are here primarily interested in the degree of hydrogen ionization and radiation losses inside the 1D slab, we use only a 5-level plus continuum hydrogen model atom. The Lα and Lβ transitions are treated with partial frequency redistribution. Once the non-LTE model has converged, we get the gas density (it must be evaluated because it depends on the ionization degree) and we can transform all structural parameters onto a geometrical $x-$scale. From these models, the radiation losses are then computed (see next subsection). Finally, we evaluate the synthetic intensities of selected hydrogen lines (Table 2) which are used for a comparison with the results of HM, of FRVG and those obtained from observations.

4.1. Radiation losses in the cool part

Once we have the converged non-LTE model of the prominence slab, the radiation losses in all hydrogen transitions

Table 1. List of models for the cool part

Model	M (g cm^{-2})	$\overline{p}$ (dyn cm^{-2})	D (km)	B_x (G)	B_{z1} (G)
M1T6	1.8 - 4	0.5	2000	6.9	4.3
M1T8	1.8 - 4	0.5	2500	6.9	4.3
M2T6	3.3 - 5	0.1	2000	3.0	1.9
M2T8	3.3 - 5	0.1	2500	3.0	1.9
M3T6	1.8 - 5	0.05	2000	2.2	1.4
M3T8	1.8 - 5	0.05	2500	2.2	1.4
M4T6	3.6 - 5	0.5	400	1.4	4.3
M4T8	3.6 - 5	0.5	500	1.4	4.3
M5T6	6.7 - 6	0.1	400	0.6	1.9
M5T8	6.7 - 6	0.1	500	0.6	1.9
M6T6	3.3 - 6	0.05	400	0.4	1.4
M6T8	3.3 - 6	0.05	500	0.4	1.4

Table 2. Radiation properties of all models. I_0 is central line intensity, I_p peak intensity for lines with self-reversal, E total line energy. Units: erg s^{-1} cm^{-2} sr^{-1} Hz^{-1}, resp. erg s^{-1} cm^{-2} sr^{-1}

.

	Lα			Lβ			Hα		
Model	I_o	I_p	E	I_o	I_p	E	I_o	I_p	E
M1T6	1.70-8	5.19-8	4.42+4	1.88-10	2.74-10	2.55+2	3.50-6	—	1.82+5
M1T8	1.81-8	6.33-8	9.47+4	2.26-10	4.86-10	8.67+2	5.16-6	7.16-6	4.82+5
M2T6	1.30-8	1.82-8	2.60+4	1.15-10	—	1.01+2	2.01-6	—	7.42+4
M2T8	1.34-8	2.16-8	3.05+4	1.21-10	—	1.16+2	2.51-6	—	1.07+5
M3T6	1.24-8	1.56-8	2.22+4	1.00-10	—	7.73+1	1.27-6	—	4.34+4
M3T8	1.27-8	1.79-8	2.30+4	1.04-10	—	8.37+1	1.32-6	—	4.91+4
M4T6	1.43-8	2.56-8	2.97+4	1.37-10	1.38-10	1.32+2	2.28-6	—	8.71+4
M4T8	1.53-8	3.45-8	4.67+4	1.54-10	1.79-10	2.03+2	3.62-6	—	1.92+5
M5T6	1.20-8	1.44-8	1.75+4	8.67-11	—	5.01+1	6.43-7	—	2.09+4
M5T8	1.22-8	1.69-8	1.82+4	8.98-11	—	6.60+1	6.96-7	—	2.47+4
M6T6	1.17-8	1.36-8	1.32+4	7.69-11	—	4.99+1	2.90-7	—	9.23+3
M6T8	1.18-8	1.57-8	1.33+4	7.86-11	—	5.31+1	2.67-7	—	9.23+3

(lines and continua) can be evaluated consistently with the internal radiation fields and atomic level populations, using the general formula for radiation-flux divergence (Mihalas 1978)

$$L = 4\pi \int_0^\infty [\eta(\nu) - \chi(\nu)J(\nu)]d\nu, \qquad (13)$$

where $\eta(\nu)$ and $\chi(\nu)$ are total emissivities and opacities, respectively, and $J(\nu)$ is the mean intensity of the radiation field. Note that in order to get accurate values of L the whole non-LTE model must have converged to high accuracy (otherwise spurious losses can appear, in particular in the central parts of the slab). However, the *total* radiation losses due to hydrogen plus all other chemical elements are more difficult to evaluate. For this we adopt a procedure which is quite usual in the literature (e.g. Kuin & Poland, 1991) and which takes optically-thin losses as given for example by Cox & Tucker (1969) or similar ones (many others have been computed since the work of these authors), removes the hydrogen contribution and replaces it by non-LTE values computed according to Eq. (13). For prominences this approach was also used by FRVG and we actually adopt their curve for optically thin losses corresponding to Cox & Tucker (1969) with hydrogen removed. For these losses, the elements He, C, N, O, Ne, Mg, Si and S are all included. Note that Kuin & Poland (1991) computed explicitely the contributions from the He atom and thus removed its optically thin counterpart. Helium does not seem to be a significant coolant at the temperatures we consider here for the cool part and thus we just take the optically thin contribution which is anyway negligible compared to hydrogen. A more serious question is the possible contribution from CaII or even MgII ions, which are important coolants in the solar chromosphere (Vernazza et al., 1981). This question was also raised by Kuin & Poland (1991) and thus we have devoted a certain attention to it. Using some representative isobaric-isothermal models we have solved the non-LTE problem for a 5-level plus continuum CaII model atom (see Gouttebroze et al., 1997) and evaluated the CaII radiation losses. All of them have been found to be substantially smaller than the hydrogen losses for the same model. This preliminary result is also consistent with findings of Zhang and Fang (1987).

5. Results for cool part

For the non-LTE modelling of the cool part of the prominence (or an individual thread) we have considered several KS-type models with the kinetic temperature varying according to Eq. (12). The basic parameters of these models are summarized in Table 1. All models are calculated for $\gamma = 40$, which simulates reasonably well the temperature profiles, and with $p_0 = 10^{-2}$ dyn cm^{-2}. In Figs. 1-6 we display, for each pair of models T6 and T8, the depth variations of six quantities (only one half of the symmetrical slab is shown):
temperature [K], gas pressure [dyn cm^{-2}], gas density [g cm^{-3}], ionization degree (the ratio of the electron (=proton) density to total hydrogen density), total radiation losses [erg s^{-1} cm^{-3}] and the divergence of the conductive flux [erg s^{-1} cm^{-3}]. All quantities are plotted against the computed geometrical scale (here x-scale in km).

Our models span a large range of possible slab configurations. We have calculated very thin slabs which could represent the basic elements of prominence fine structures. We have also constructed thick slabs to model more uniform prominences without much fine structure. In all our models the central gas pressure is much higher than the pressure in the ambient corona. The pressure profile given in Eq. (2) is a direct consequence of the assumed magneto-hydrostatic equilibrium. On the other hand the temperature profile which we have taken (see Eq. (12)) has no direct physical basis. We only required that the temperature is sufficiently uniform in the central parts and then rises steeply towards the boundary of the inner region, which is normally observed. As one can see from our figures the temperature increase from, say 10000 K to 30000 K occurs in some of our models over an extended region, but the total mass contained in these regions is rather small. In principle we could make all temperature profiles steeper by selecting appropriate values of the exponent γ. But this is beyond the scope of the present paper.

5.1. Energy balance

From Figs. 1-6 we can draw several important conclusions regarding the energy balance. First, we get the depth variations of radiation losses L which exhibit two characteristic peaks. The central peak is dominated by non-hydrogenic losses for models with $T_{cen} = 6500$ K, hydrogen contribution is small and even negative at this temperature - see Figs. 7 and 8. For $T_{cen} = 8000$ K, the central peak still contains a substantial contribution by non-hydrogenic losses, but the hydrogen losses are now positive and are of the same magnitude as other losses (Figs.7 and 8). For $T = 8000$ K this means that the amount of losses considered for the energy balance at central parts of the

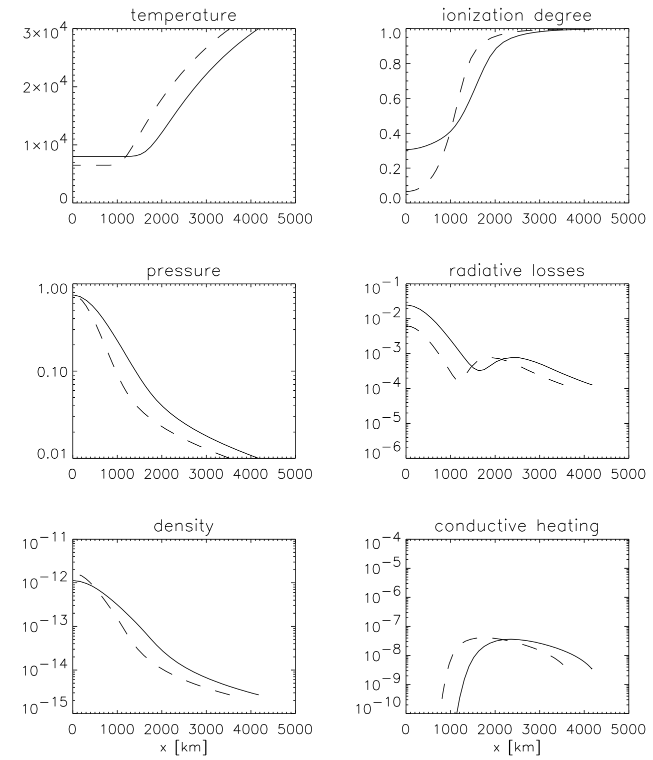

Fig. 1. Depth variations of different parameters inside the prominence and the inner part of the PCTR, for models M1T6 and M1T8. Solid lines: $T_{cen} = 8000$ K, dashed lines: $T_{cen} = 6500$ K. All quantities (with the exception of the x-coordinate) are in cgs units.

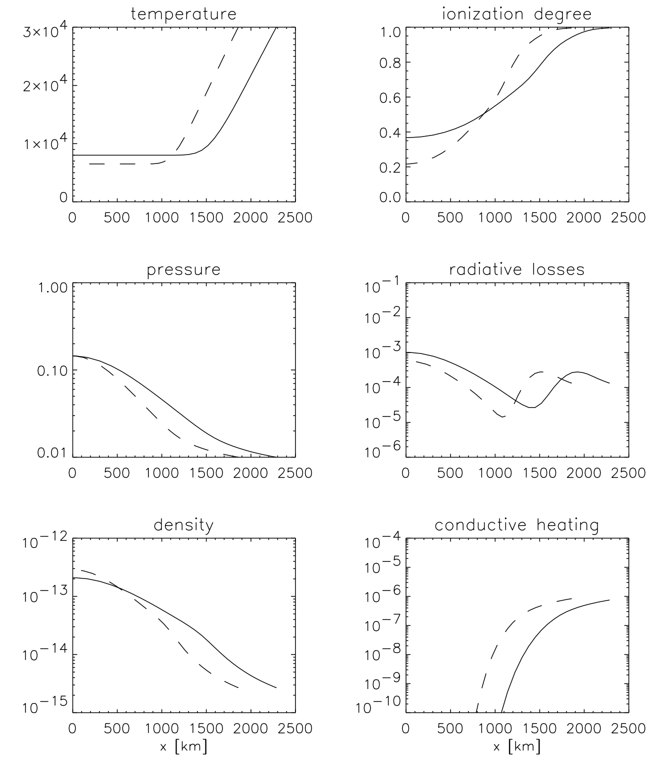

Fig. 2. Same as figure 1 but for models M2.

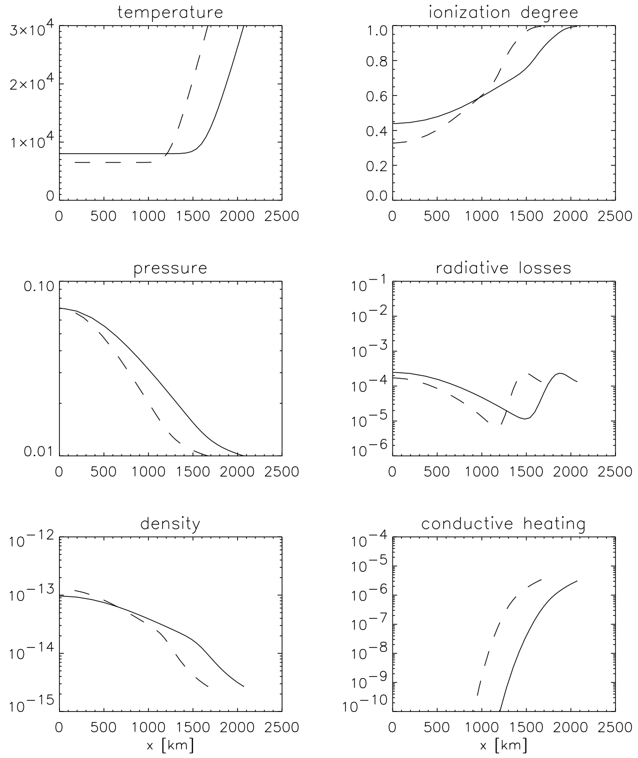

Fig. 3. Same as figure 1 but for models M3.

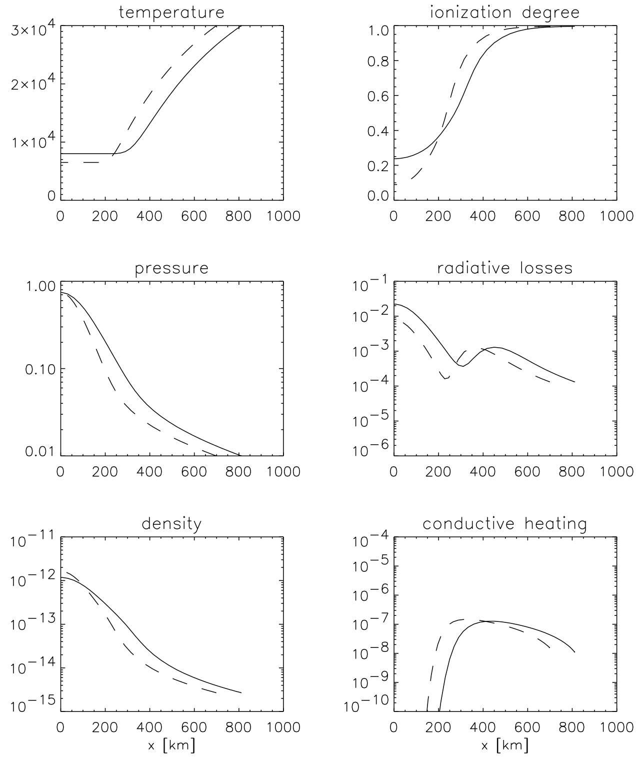

Fig. 4. Same as figure 1 but for models M4.

slab has important hydrogenic component which we here compute in detail. The non-hydrogenic component, which is approximated by optically-thin losses, is less accurate. If the latter one would be in reality smaller, the total losses will be changed only by a factor of two and this still requires a substantial heating in the central parts. On the other hand, for higher non-hydrogenic losses we need even more heating. The central peak is due to a maximum of the gas density at the slab center. However, apart from a strong temperature dependence, the losses are proportional to $n_e n_H$ (electron and hydrogen density), which in turn depend on both ρ and the ionization degree.

The second peak is due to hydrogen, namely the Lα line. The formation of this peak corresponds to the region where the Lα line core is formed and the width of such a region represents the layer in which Lα is effectively thin. In this region the Lα line source function S is almost completely decoupled from the local Planck function $B(T)$. In the central parts of the slab S tends towards thermalisation, but full thermalisation, i.e. $S = B(T)$, is reached at the slab center only for those of our models which have the largest mean pressure and geometrical extension. Note also that the peak due to Lα coincides with the region where the ionization degree reaches unity. A similar Lα peak also exists in the upper solar chromosphere (Vernazza et al., 1981).

Maximum total losses reach values around 10^{-2} erg s^{-1} cm^{-3}, at the center of slabs which have the highest pressures considered. Total radiative losses are positive for all our models at all depths.

Since all these losses have been computed assuming a 'semiempirical' type of the temperature profile, they naturally represent the total amount of heating required to obtain the prescribed $T(x)$, according to Eq. (11). The first question which arises is whether the divergence of the thermal conductive flux is capable of balancing these losses. The answer is definitely no, which is obvious from all our figures. The conductive heating term computed from Eq. (1) (we have taken into account the geometry of the magnetic field) is typically several orders of magnitude smaller than L. Only for some models with very small geometrical thickness this heating can reach the radiation losses, a situation met in the extremely narrow models of FRVG. Note that in some cases, depending on the temperature gradient at the base of PCTR (i.e. our parameter γ), the divergence of conductive flux is even negative, which means cooling by conduction. However, all these values are very small and thus negligible. At the slab center, the conductive heating goes to zero. This can be shown analytically for our class of temperature profiles, provided that the exponent $\gamma \geq 2$.

For very narrow slabs, with steep temperature gradients and a constant pressure (i.e. isobaric models), FRVG were able to construct energy-balance models just by adding the ambipolar diffusion heat flux divergence and neglecting any kind of additional heating. However, in our models, a substantial heating is required because our tem-

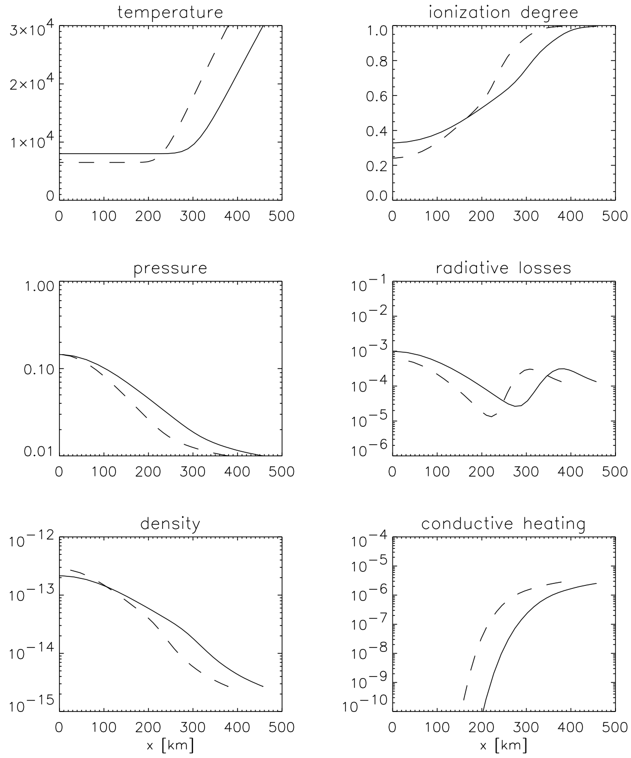

Fig. 5. Same as figure 1 but for models M5.

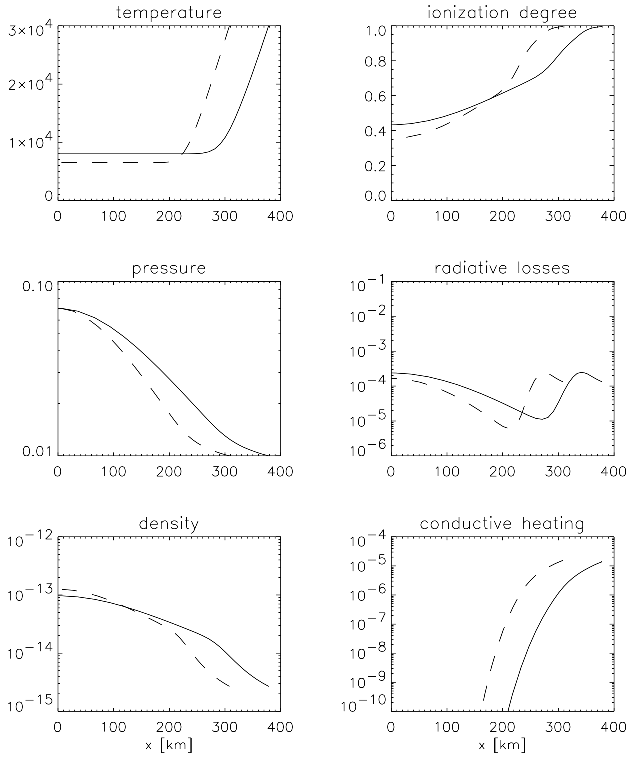

Fig. 6. Same as figure 1 but for models M6.

perature gradients are insufficient to ensure effective conductive heating even for the case that ambipolar diffusion is included.

5.2. Output radiation intensities

In Table 2 we summarize the output (synthetic) line intensities for Lα, Lβ and Hα lines. Both Lyman lines were computed using the partial frequency redistribution. We see a large variety of intensities and peak-to-center ratios, depending on the model. Most of Lα profiles are consistent with observations. Lβ integrated intensities are still smaller than OSO-8 data (see Heinzel et al., 1987 and FRVG), but for some models they reach values comparable to recent observations by SOHO/SUMER (Schmieder et al., 1999). Our models predict much lower Lβ intensities than those of FRVG. Very high intensities computed by FRVG are explained by the importance of the ambipolar diffusion. Since our temperature structure is 'semiempirical', the ambipolar diffusion could play a role only in the statistical equilibrium equations via the advection terms which we neglect here (in fact, using the FRVG models, we were unable to reproduce their high Lβ intensities). Our Hα integrated intensities are also in the range of the observed values.

The Balmer decrement computed from our models, using the 5-level hydrogen model atom, is similar to that obtained by HM. However, their criticism of KS-type models which *'predict the Balmer decrement different from mean observed values'* is misleading. First, for a 5-level hydrogen atom the intensities of Hβ and Hγ lines are underestimated as was demonstrated by Gouttebroze et al. (1993). Second, a 'mean' Balmer decrement is, by definition, a value which lies out of the relation presented e.g.

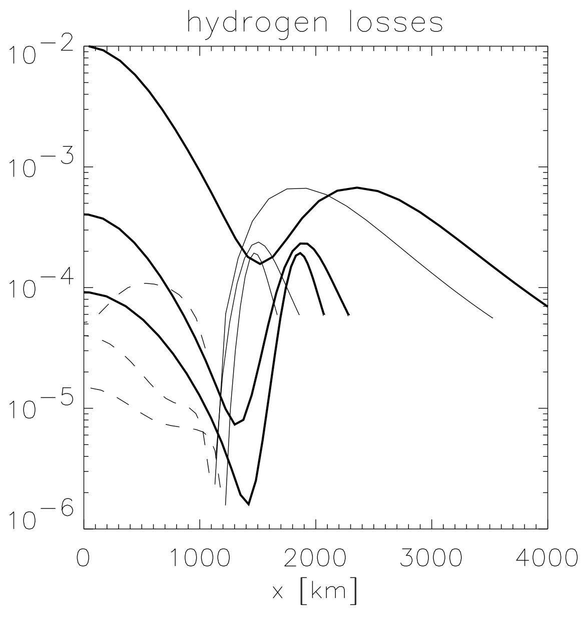

Fig. 7. Hydrogen losses for models M1T8 to M3T8 (thick solid lines) and models M1T6 to M3T6 (thin lines, dashed thin lines indicate radiative gains).

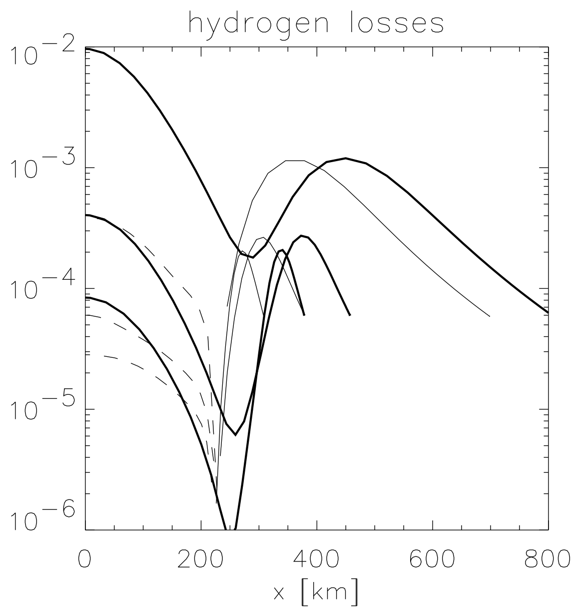

Fig. 8. Same as figure 7 but for models M4T8 to M6T8 and M4T6 to M6T6.

by Heinzel et al. (1994). Therefore, any comparison of the computed Balmer decrement with a 'mean' observed value is meaningless.

A more systematic study of the radiation properties of our models will be the subject of a future paper where we plan to investigate the role of the parameter γ on the width of PCTR and thus on the shape of Lyman lines. We also intend to consider the effects resulting from several slabs (threads) along the line of sight, as in FRVG.

6. The prominence-corona transition region

This region is modelled by making the following simplifying assumptions: we take a constant gas pressure and use the optically thin approximation for radiation losses. For the loss function we take Hildner's (1974) formula of piece-wise power laws given by

$$L = p^2 \chi_i T^{\alpha_i - 2}, \tag{14}$$

where p is the gas pressure and the quantities χ_i and α_i are tabulated by Hildner (1974). We have used the approximate relation

$$p = 2 n_e k T \tag{15}$$

and again take cgs units. We model only the region 20000 K $\leq T \leq 10^6$ K in which L is a monotonically decreasing function of T; but this only holds for the special case of p=const.

As has been described earlier, the heating mechanisms of the transition region and the corona are not yet understood and the heating functions are unknown. For this reason we have adopted the following approach: we choose some very simple parametric representations for this heating function and then solve numerically the differential equation (1) to obtain the temperatur profile $T(x)$. The calculated profiles then will give us constraints on the possible heating functions. This is similar to the approach taken by Chiuderi and Chiuderi Drago (1991).

For a first guess we took

$$H = a L(T_1) \left(\frac{T_1}{T}\right)^{\mu} \tag{16}$$

with $T_1 = 20000$ K, a and μ being free parameters, $a < 1$ and $\mu \geq 0$. In all our PCTR and coronal models we also assume B_x/B = const., contrary to the cool inner part. We then integrate the second-order differential equation (1) between $x_1 = 0$ and $x_2 = 10^{10}$ cm, where x_1 denotes the position of the boundary between prominence and transition region. As initial values at x_1 we take $T = T_1$ and $(dT/dx) = U$. The slope of $T(x)$ at x_1 is taken as a free parameter. It is found that the behaviour of the solutions does not depend strongly on the exact value of U, as long as $U < 10^{-2}$ K/cm holds.

Our solutions will then depend on the following set of parameters:

1. The field line inclination B_x/B
   This represents a constant multiplying factor on the left hand side of Eq. (1) which can be included in the definition of the length scale. Therefore, we shall perform all calculations for $B_x/B = 1$ and then rescale the x-coordinate by the factor B_x/B.
2. The gas pressure p
   Since in our models both L and H are proportional to p^2, the quantity $1/p$ has the same property as B_x/B for Eq. (1). For this reason we take $p = 0.02$ dyn cm^{-2}. The solutions for any other value p' can then be found by multiplying x by the ratio p/p'.
3. The parameters a and μ which define the heating function

Of major interest is the position where the heating function crosses the loss function. If this crossing occurs at low temperatures then the maximum temperature will be much less than 10^6 K and the width of the entire transition zone becomes very small. Therefore sufficiently high crossing temperatures are needed. One sees that this crossing temperature increases with decreasing a and increasing μ.

We have performed a parameter study for the values of a and μ and we show some representative temperature profiles in Figs. 9 and 10; all the curves are given for p = 0.02 dyn cm^{-2} and $B_x/B = 1$ as mentioned above.

Fig. 9 shows the temperature profiles for the cases with $a = 0.03$, $\mu = 0$ (full line), $a = 0.005$, $\mu = 0$ (dashed line), $a = 0.2, \mu = 1$ (dot-dash line) and $a = 0.5, \mu = 1.5$

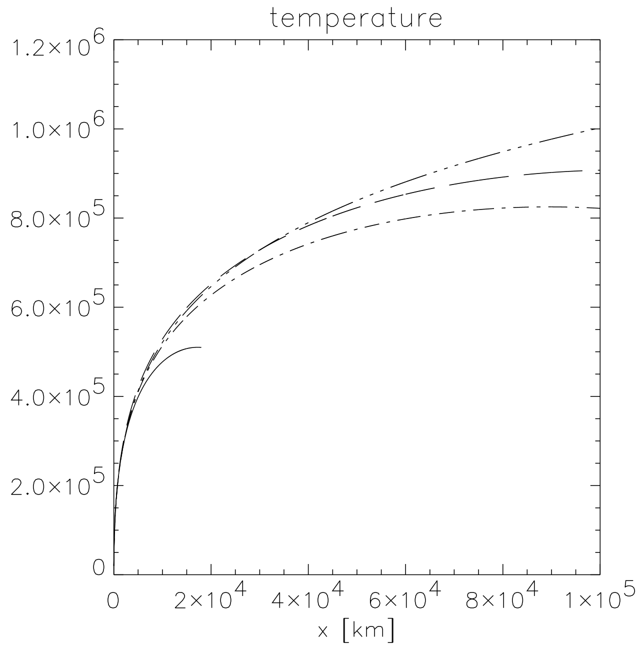

Fig. 9. Temperature profiles for the outer parts of the transition region for different types of heating functions (see text). Note: origine of x-coordinate has been shifted to position where T=20000 K holds.

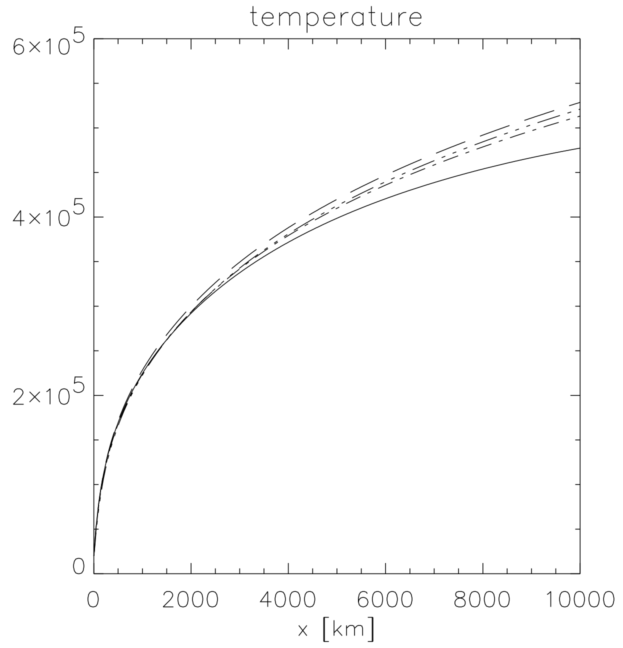

Fig. 10. Blow-up of the inner region of figure 9.

(trippledot-dash line). Fig. 10 is a blow-up of the innermost part of the transition region. This special selection of models shows that a variety of heating functions can give acceptable forms for the global temperature profile in the transition zone. Note that the situation is different from that in the cool parts. The inner part has strongly vary-

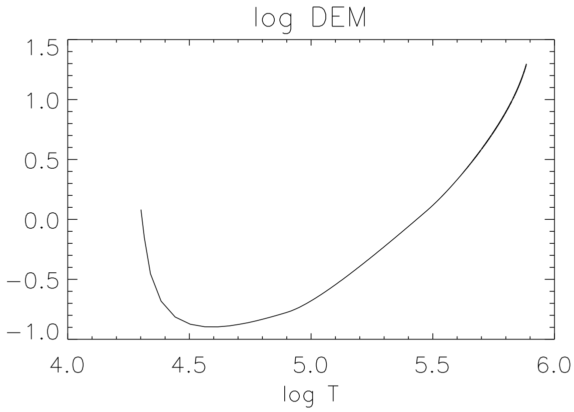

Fig. 11. Calculated differential emmission measure for a model with a=0.99 and μ=1.5.

ing gas pressure and the losses are not optically thin. This, together with an arbitrarily prescribed heating function, could produce unrealistic temperature profiles. Therefore, we have used in those cool regions a different concept of a 'semiempirical' temperature structure as already discussed above.

If the vertical sagging of the field lines and the shearing is taken into account then B_x/B will lie somewhere in the range 0.2 to 0.5. This then will result in a reduction of the transition region width by this same factor. If the coronal gas pressure is larger than 0.02 dyn cm^{-2} then this will lead to an even larger reduction of the transition region width, whereas a smaller value of p gives a larger transition region.

An important quantity which is obtained from our modelling is the differential emission measure (DEM) defined as

$$DEM = p^2 \left(\frac{dT}{dx}\right)^{-1} . \tag{17}$$

This quantity can be compared with observed curves for the DEM as given for example in Engvold et al. (1987). Fig. 11 shows the theoretical DEM curve for a model with $a = 0.99$ and $\mu = 1.5$. By comparing our curve with the measurements of Engvold at al. (1987), one finds that these theoretical values are of the right order of magnitude. However, the minimum is not at the expected position. The observations require $T_m \simeq 10^5$ K whereas our curve has $T_m = 40000$ K. If we use some other values for the parameters a and μ in our heating function then the differences between our models and the the observed DEM curve become even larger.

Chiuderi & Chiuderi Drago (1991) suggested that an extremely fine tuning of the heating function could give a sufficiently good agreement. But whether or not this assumption is reasonable is still an open question. Here we only want to point out that the basic energetics of the transition region seems to be correct but the details will require further studies.

Our models for the hot part of the PCTR start at $T = 20000$ K whereas the models of the cool inner part presented in the previous section extend to 30000 K. Therefore, we have a certain overlap between the two sets of models. But since the physical assumptions made for these two parts are different, the models do not give exactly the same results in this region of overlap. In particular, the temperature gradients are different in both kinds of models. The fits could be improved by taking a different temperature variation in the inner region (parameter γ in Eq. (12)), as well as a different heating function in the outer part. But since this region of overlap is small both in space and temperature regime, we have ignored these differencies in the present investigation.

7. Discussion and conclusions

Our models require that some form of additional heating balances the radiative losses inside the prominence. From all these models we see that the heating function has to increase from the low values in the outer parts to higher ones for the prominence interior. Depending on the optical thickness of the prominence, the maximum heating either has to occur at the center of the prominence slab or in the Lα formation region. The picture becomes different when one considers the heating which is required *per gramm* of material. Then the heating in the center of the prominence is typically by a factor 5 – 100 smaller than that at the boundary (i.e. at 30000 K) for all our models. From this we conclude that any type of coronal heating which provides enough energy at a temperature of 30000 K should also be sufficient to heat the inner parts.

Possible heating mechanisms are the dissipation of Alfvén waves or the reconnection of magnetic fieds. For the Alfvén wave heating it is necessary that these waves can penetrate deep enough into the prominences. Magnetic reconnection could result from the fact that the prominence weight can induce large currents inside the prominence and also that there the plasma has a low temperature as compared to the surrounding corona. If prominences are not completely static then heating by enthalpy inflow can also play a major role as has been pointed out by Poland & Mariska (1986). The energy-balance models of HM and FRVG are quite different from our models. HM use the KS-type pressure balance as we do, but they assume radiative equilibrium to get the temperature structure. This leads to rather low temperatures in the center of the slab (for some magnetic models is below 5000 K) and no PCTR. However, the general conclusion of HM that these magnetohydrostatic models are unrealistic is not acceptable. Apart from the temperature structure they derive, these models represent correct pressure-equilibrium solutions. The fact that HM get very narrow slabs is due to their unrealistically high coronal pressure. Finally, the Balmer decrement if computed with a realistic hydrogen atom model (with more than 5 levels) should be consistent with typical observations. FRVG, on the other hand, assume an isobaric slab and solve the energy-balance equation for the temperature structure. The reason why these authors get extremely narrow slabs (a few tens of km) is that they consider only the conductive heating (including the ambipolar diffusion). In the central parts, where the temperature gradient goes to zero (for symmetry reasons), this kind of heating is small and thus very narrow slabs with enhanced temperature gradients are needed to keep the central temperature at the value 6500 K. In our models, the same central temperature has to be balanced by extra heating because the conduction is quite inefficient.

It seems that the available heating mechanisms can provide the energy in a global way and for this reason the prominence when considered as a whole will be in thermal equilibrium. But in our models there is also the requirement that the heating balances the losses locally at each position within the prominence. This implies that the heating as a function of temperature and density has to be well tuned. One can then speculate that in the case that such a local balance is not achieved throughout the entire prominence, some small scale motions which have been observed in many prominences could transport the energy from one place to another. Such a process would lead to a situation where the energy equilibrium is only obtained in an averaged sense, while locally the situation will be highly dynamical.

Such a fine-tuning is not required for the hotter parts of the PCTR because in these regions thermal conduction can supply, or remove, the appropriate amount of energy at any position. For this reason we were able to construct a series of PCTR models for different types of heating functions. One has, however, to bear in mind that there is the additional constraint that realistic models should reproduce also the observed DEM curves. The temperature profiles in the inner regions which we have chosen somewhat arbitrarily can be constrained by making use of the optical and UV spectral observations in different lines of different chemical species. In particular, for the base of the PCTR, the newly obtained SOHO/SUMER observations of hydrogen Lyman lines and continuum are very promising (Schmieder et al., 1999). This type of consideration could also be extended to the outer regions if one uses high-temperature spectral lines. This then will give some clues about the heating mechanisms. However, all these aspects go beyond the scope of the present paper and will be postponed to future investigations.

Acknowledgements. PH acknowledges the support and hospitality of the MPA in Garching where most of this study was done. The support of the Ondřejov observatory during the visit of UA is also appreciated. This work was partly supported by the grant A3003902 of the Academy of Sciences of the Czech Republic. We would also like to thank Friedrich Meyer and the referee, Pascal Démoulin, for their kind help to improve the presentation of our paper.

References

Anzer U., 1995, Solar Phys. 161, 49
Anzer U., Heinzel P., 1998, Solar Phys. 179, 75
Chiuderi C., Chiuderi Drago F., 1991, Solar Phys. 132, 81
Chiuderi Drago F., Engvold O., Jensen E., 1992, Solar Phys. 139, 47
Cox D.P., Tucker W.H., 1969, ApJ 157, 1157
Engvold O., Kjeldseth-Moe O., Bartoe J.-D.F., Brueckner G.E., 1987, In: Small-Scale Plasma Processes, Eds. Battrick B., Rolfe E.J., ESA SP-275, p.21
Engvold O., Hirayama T., Leroy J.-L., Priest E.R., Tandberg-Hanssen E., 1990, In: Dynamics of Quiescent Prominences, Eds. Ruždjak V., Tandberg-Hanssen E., Lecture Notes in Physics 363, Springer, p.284
Fontenla J.M., Rovira M., Vial J.-C., Gouttebroze P., 1996, ApJ 466, 496 (FRVG)
Gouttebroze P., Heinzel P., Vial, J.-C., 1993, ApJS 99, 513
Gouttebroze P., Vial, J.-C., Heinzel, P., 1997, Solar Phys. 172, 125
Heasley J.N., Mihalas D., 1976, ApJ 205, 273 (HM)
Heinzel P., 1995, A&A 299, 563
Heinzel P., Anzer U., 1998, In: New Perspectives on Solar Prominences, IAU Coll. 167, Eds. Webb D., Rust D., Schmieder B., ASP Conf. Ser. Vol. 150, p.213
Heinzel P., Anzer U., 1999, in preparation
Heinzel P., Gouttebroze P., Vial J.-C., 1987, A&A 183, 351
Heinzel P., Gouttebroze P., Vial J.-C., 1994, A&A 292, 656
Hildner E., 1974, Solar Phys. 35, 123
Kippenhahn R., Schlüter A., 1957, Z. Astrophys. 43, 36 (KS)
Kuin N.P.M., Poland A.I., 1991, ApJ 370, 763
Low B.C., Wu S.T., 1981, ApJ 248, 335
Mihalas D., 1978, Stellar Atmospheres, 2nd ed., Freeman & Co., San Francisco
Paletou F., 1995, A&A 302, 587
Poland A.I., Anzer U., 1971, Solar Phys. 19, 401
Poland A.I., Mariska, J.T., 1986, Solar Phys. 104, 303
Schmieder B., Kucera T., Heinzel P., Vial J.-C., 1999, In: Proc. SOHO-8 Workshop, Paris, ESA SP, in press
Tandberg-Hanssen E., 1995, The Nature of Solar Prominences, Kluwer Academic Publ., Dordrecht
Vernazza J.E., Avrett E.H., Loeser R., 1981, ApJS 45, 635
Webb D., Rust D., Schmieder B. (Eds.), 1997, New Perspectives on Solar Prominences, IAU Coll. 167, ASP Conf. Ser. Vol. 150
Zhang Q.Z., Fang C., 1987, A&A 175, 277